J Mater Sci: Mater Med (2011) 22:1247–1255
DOI 10.1007/s10856-011-4291-x

Improved bioabsorbability of synthetic hydroxyapatite through partial dissolution-precipitation of its surface

Xianjun Ding · Masahiko Takahata · Toshiyuki Akazawa · Norimasa Iwasaki · Yuichiro Abe · Miki Komatsu · Masaru Murata · Manabu Ito · Kuniyoshi Abumi · Akio Minami

Received: 2 December 2010 / Accepted: 11 March 2011 / Published online: 31 March 2011

Abstract Even though synthetic hydroxyapatite (HAp) has a chemical composition similar to the mineral phase of bone, it is minimally absorbed and replaced by bone tissue. This could be because HAp is composed of compactly arranged apatite crystals with homogenously large grains. In this study, the surface and non-stoichiometry of the synthetic HAp crystals was modified by partial dissolution and precipitation (PDP) to improve bioabsorbability of HAp. In vitro cell culture demonstrated that more osteoclasts were activated on PDP-HAp compared with HAp. In vivo implantation using a rabbit bone defect model revealed that PDP-HAp was gradually degraded and was replaced by bone tissue. Consistent with the in vitro results, more osteoclasts were activated in PDP-HAp than in HAp, indicating that the former was absorbed through the stimulation of osteoclastic activity. These results suggest that the PDP technique may have clinical utility for modifying synthetic HAp for use as superior bone graft substitutes.

X. Ding · M. Takahata (✉) · N. Iwasaki · Y. Abe · M. Komatsu · M. Ito · K. Abumi · A. Minami
Department of Orthopedic Surgery, Graduate School of Medicine, Hokkaido University, Kita-15 Nishi-7, Kita-ku, Sapporo 060-8638, Japan
e-mail: takamasa@med.hokudai.ac.jp

T. Akazawa
Hokkaido Research Organization, Industrial Research Institute, Industrial Technology Research Development, Local Independent Administrative Agency, Sapporo, Japan

M. Murata
2nd Department of Oral Surgery, Health Sciences University of Hokkaido, Sapporo, Japan

1 Introduction

Synthetic hydroxyapatite ceramics (HAp) is one of the most popular bone graft substitutes. It has been widely utilized in various fields, including orthopedic, craniomaxillofacial, dental, and plastic surgery, because of its excellent biocompatibility and osteoconductivity. Highly porous HAp with interconnecting pores exhibit excellent osteointegration by allowing new bone tissue to penetrate the material [1, 2]. However, despite its desirable characteristics as a bone substitute, it cannot be replaced by bone tissue due to poor bioabsorbability [3, 4].

The crystallographic properties of synthetic HAp are most likely responsible for its minimal bioabsorbability. Although the lack of biological activity slows the remodeling of material, it is not critical for its bioabsorption as in other synthetic bone substitutes such as β-tricalcium phosphate that are absorbed by the body [3, 5, 6]. Crystallographic properties such as grain size, chemical perfection, orientation, and density of HAp crystals have a decisive influence on its bioabsorbability. These properties govern the surface geometry, spatial structure, and solubility of the material, reportedly responsible for the bioabsorbability of calcium phosphate materials [7]. This is likewise supported by the fact that synthetic HAp and bone apatite have similar chemical compositions but have different crystallographic properties. Apatite crystals in bone lack chemical perfection and are arranged along collagen fibers with heterogeneous grain sizes. In contrast, synthesized HAp, typically made through sintering, is composed of compactly arranged hydroxyapatite crystals with large homogenously sized grains [8, 9]. Therefore, we hypothesize that modifying the crystallographic properties of synthetic HAp would improve its bioabsorbability.

To modify crystallographic properties of synthetic HAp, a partial dissolution-precipitation (PDP) method was developed [10]. This technique was originally developed by Akazawa et al. [11, 12] to improve the bioabsorbability of calcined HAp from bovine bone. Partial dissolution with HNO_3 etching produces microcracks, as well as renders the surface apatite grains smaller and more spherical. Precipitation treatment forms microcrystals on the surface of apatite grains. The resulting HAp ceramics have gradations in terms of degrees of crystallinity and grain size from the surface layer to the bulk structure region. The improved microstructure contributes to the bioabsorbability of calcined bovine HAp, which was completely absorbed in the subcutaneous tissues of the back region of rats 12 weeks after implantation [11].

In this study, we evaluated whether PDP treatment improves the bioabsorbability of synthetic HAp in vitro and in vivo. An in vitro osteoclastic resorption assay was performed to investigate how PDP treatment of the HAp surface affected osteoclastic activity. The in vivo study was performed using rabbit femoral condyle bone defect model to compare the bioabsorbability and osteointegration capacity of untreated and PDP-treated synthetic porous HAp.

2 Materials and methods

2.1 In vitro osteoclast culture

The in vitro osteoclastogenesis assay was performed on CELLYARD^{TM} HAp pellets (Hoya Co., Tokyo, Japan). The 13 mm diameter pellets fitted each well of a 24-well cell culture plate. The surface of the HAp pellet was modified by PDP treatment as described previously [10]. The pellets were partially dissolved in the HNO_3 solution by supersonication at 120 W and 38 kHz for 1 min. The pH of the solution was then adjusted to 10.5 by the dropwise addition of an aqueous ammonium solution to reprecipitate HAp crystals onto the surface of the pellet. The surface-modified HAp (PDP-HAp) pellet was then left to stand for 24 h, washed, and dried at 323–393 K.

Osteoclasts were generated by co-cultures of murine primary osteoblasts and bone marrow cells [13]. The primary osteoblasts were obtained from the calvaria of newborn C57BL/6 mice by digestion using 0.1% type II collagenase and 0.2% dispase dissolved in phosphate buffered saline. The cells were grown in alpha-minimum essential medium supplemented with 10% fetal bovine serum, 100 IU/ml penicillin G, and 100 μg/ml streptomycin (Meiji Seika, Tokyo, Japan). Mouse bone marrow cells were isolated from the femora and tibiae of C57BL/6 male mice 6–9 weeks old. The bone marrow cells (1×10^6 cells/well) were then mixed with primary osteoblasts (2×10^5 cells/well) and seeded onto 24-well plates with either a PDP-HAp or a HAp pellet in each well. These were subsequently cultured with 10 nM 1,25-dihydroxyvitamin D3 and 100 nM prostaglandin E2. The medium was changed every 3 days up to day 12 of the culture period. Osteoclast formation and bone absorption were assessed on day 12 by tartrate-resistant acid phosphatase (TRAP) staining and mRNA expression analysis.

2.2 TRAP staining of cultured HAp pellets

The surface of the treated HAp pellets were fixed and stained to identify osteoclasts and resorption pits using a TRAP histochemical kit (Hokudo, Co., Ltd., Japan) according to the manufacturer's instructions. After staining, the surfaces of HAp and PDP-HAp pellets were observed under a stereomicroscope. The TRAP-stained areas of three different pellets from the HAp and PDP-HAp treatments were measured and compared using Image J software (NIH).

2.3 mRNA expression of osteoclast and osteoblast marker genes

To analyze osteoclast and osteoblast markers, the total RNA of cultured cells was isolated using the RNeasy Mini Kit according to the manufacturer's instructions (Qiagen, Valencia, CA). cDNA was synthesized from 1 μg of total RNA using reverse transcriptase and oligo-dT primers. Quantitative real-time polymerase chain reaction was then performed using the DNA Engine Opticon 2 System (MJ Research, Hercules, CA). The 2× SYBR Green Mastermix (DyNAmo^{TM} HS SYBR Green qPCR Kit, Finnzymes Oy, Finland) was used to amplify and detect the target genes.

cDNA samples were analyzed for both the genes of interest and the reference gene (glyceraldehyde-3-phosphate dehydrogenase; GAPDH). The primer sequences used to amplify mouse calcitonin receptor (CTR), cathepsin K (CTSK), integrin $\beta 3$ (ITG$\beta 3$), TRAP, receptor activator of nuclear factor-κB ligand (RANKL), alkaline phosphatase (ALP), osteocalcin (OC), and GAPDH are presented in Table 1. Cycle threshold values were obtained graphically. The relative mRNA expression of each targeted gene was normalized with the cycle threshold values of GAPDH.

2.4 Preparation of PDP-HAp implant for in vivo experiment

Commercially available synthetic HAp with 85% porosity and interconnecting pores (HAp; APACERAM AX, Hoya Co., Tokyo, Japan) was used as the starting material. After being cut into 5 mm × 5 mm × 5 mm cubes, the samples

Table 1 Sequence of primers used in quantitative RT-PCR

Gene	Forward primers (5′–3′)	Reverse primers (5′–3′)	Product length (bp)	Accession number
CTR	TGG CTG TGT TTA CCG ACG AG	CGA GTG ATG GCG TGG ATA AT	146	NM_007588
CTSK	TGGATGAAATCTCTCGGCGT	TCATGTCTCCCAAGTGGTTC	123	NM_007802
ITGβ3	TGACTCGGACTGGACTGGCTA	CACTCAGGCTCTTCCACCACA	414	NM_016780
TRAP	AGTCCTGCTTGTCCGCTAAC	AGAGAAGCTGCCGTGAGTGA	96	NM_007388
RANKL	GGCCAAGATCTCTAACATGA	TAGTCTGTAGGTACGCTTCC	126	NM_011613
ALP	TCCGTGGGCATTGTGACTA	CTGGTGGCATCTCGTTATCC	106	NM_007431
OC	GACCGCCTACAAACGCATC	GAGGATCAAGTCCCGGAGAG	104	NM_007541
GAPDH	ACTTTGTCAAGCTCATTTCC	TGCAGCGAACTTTATTGATG	269	BC_098095

were partially dissolved in HNO_3 solution by supersonication at 120 W and 38 kHz for 25 min. The hydroxyapatite nanocrystals were then reprecipitated onto the surfaces and pore walls of the HAp samples at 298 K through the gradual addition of an NH_3 solution until the pH reached 10.5. The modified HAp was left to stand for 24 h, washed, and dried at 323–393 K to produce PDP-HAp ceramics. Scanning electron microscope (SEM) micrographs of the HAp and PDP-HAp ceramics were taken to confirm their morphology and microstructure.

2.5 Operative procedures

The experimental protocol of the animal study was reviewed and approved by the Institutional Animal Care and Use Committee. A total of 24 female Japanese white rabbits, 4–5 months old, weighing 3.0–3.5 kg, were used for this study. General anesthesia was induced with an intravenous administration of sodium pentobarbital (20 mg/kg) and maintained with 2% isoflurane. Benzylpenicillin potassium (Penicillin G potassium, Meiji Seika, Tokyo, Japan) was injected at 5000 U/kg into the quadriceps muscle for prophylaxis prior to surgery. Under sterile conditions, the medial condyle of the femur was exposed through a medial longitudinal skin incision. A 5 mm × 5 mm × 5 mm square bone defect was created in the medial condyle of femur bilaterally by a surgical drill and surgical knife (Fig. 1a). The orientation of defects was perpendicular to the sagittal axis of the femur (Fig. 1c). The defects were flushed with sterile saline to remove bone debris prior to being filled with bone graft substitutes to the height of the original cortex. A block of either HAp or PDP-HAp was implanted into the bone defects of the right or left femur (Fig. 1b). The wound was closed sequentially by layer.

All rabbits were housed individually in cages and allowed an ad libitum diet and water. Eight rabbits each were sacrificed at 4, 8, and 16 weeks after the operation and both femurs were harvested with the surrounding soft tissue. The distal portions of both femurs were carefully retrieved and subjected to postmortem analyses. Samples at 4, 8, and 16 weeks were all examined by radiography and micro-computed tomography (CT) scanning. The samples collected at weeks 4 and 16 were evaluated histologically and histomorphometrically. Week 8 samples were unavailable for histological evaluation due to a technical problem encountered during histological preparation.

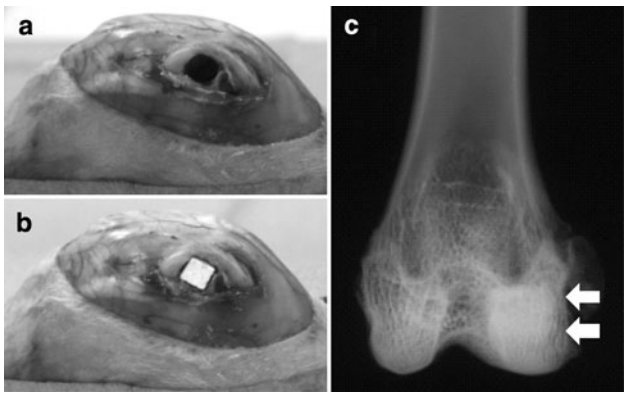

Fig. 1 The operative procedure. **a** Bone defects (5 mm × 5 mm × 5 mm) were created in the medial condyle of bilateral femurs using a surgical drill and knife. Orientation of the defect was perpendicular to the sagittal axis of the femur. **b** Either a block of HAp or PDP-HAp (5 mm × 5 mm × 5 mm) was implanted into the bone defect. **c** Radiographs were taken to confirm the position and orientation of the implants. *Arrows* indicate the location of the implant

2.6 Assessment by X-ray and Micro-CT

Radiographs of the distal portion of femur were taken at 40 kV and 4 mA for 120 s using a soft X-ray apparatus (SRO-M50D; Tanaka X-ray, MFG Co. Ltd., Tokyo, Japan) to confirm the position and condition of the implants. Micro-CT scanning in the axial plane was performed using a μCT scanner (MCT-CB100MF; Hitachi Medical, Tokyo, Japan) to evaluate implant resorption and corresponding bone formation.

2.7 Histology

The specimens were fixed with 70% ethanol at 4°C for 1 week. The undecalcified specimens were then embedded

in glycol methacrylate resin and sectioned axially at 5 μm. The sections were mounted onto glass slides, stained for TRAP activity with toluidine blue O and observed under light microscopy. The preimplantion materials were similarly treated for comparison.

2.8 Histomorphometry

To assess implant material degradation and bone ingrowth after the surgery, the volume of residual HAp materials and the amount of bone tissue inside the implant were measured using the histological sections. The following measurements were made: HAp area/total area (H.Ar./T.Ar. %), porosity, pore size, bone area/total area (B.Ar/T.Ar. %), bone contact surface/total surface (B.C.S./T.S.), and number of osteoclasts (N.Oc). To evaluate these parameters, the ceramics and biological bone area were isolated according to difference in color using the imaging software of Image J (NIH). The black areas represent the ceramic material and blue areas represent calcified bone. The H.Ar./T.Ar. and pore size were measured by analyzing micrographs of the isolated ceramics, whereas B.Ar/T.Ar. was measured from the micrographs of the isolated bone. B.C.S./T.S. was calculated as the perimeter of the material in contact with the newly formed bone divided by the total perimeter of material. N.Oc was calculated for each sample using five 1 mm^2 rectangular areas, four designated at the corners and one in the center of the materials. Osteoclasts were defined as TRAP-positive cells with three or more nuclei.

2.9 Statistical analysis

Data are expressed as mean ± SD. Statistical differences were evaluated with the Student's paired *t*-test and P value < 0.05 was considered significant.

3 Results

3.1 In vitro osteoclastogenesis assay

The surfaces of both the HAp and PDP-HAp pellets appeared to have numerous TRAP-stained dots (Fig. 2a, b).

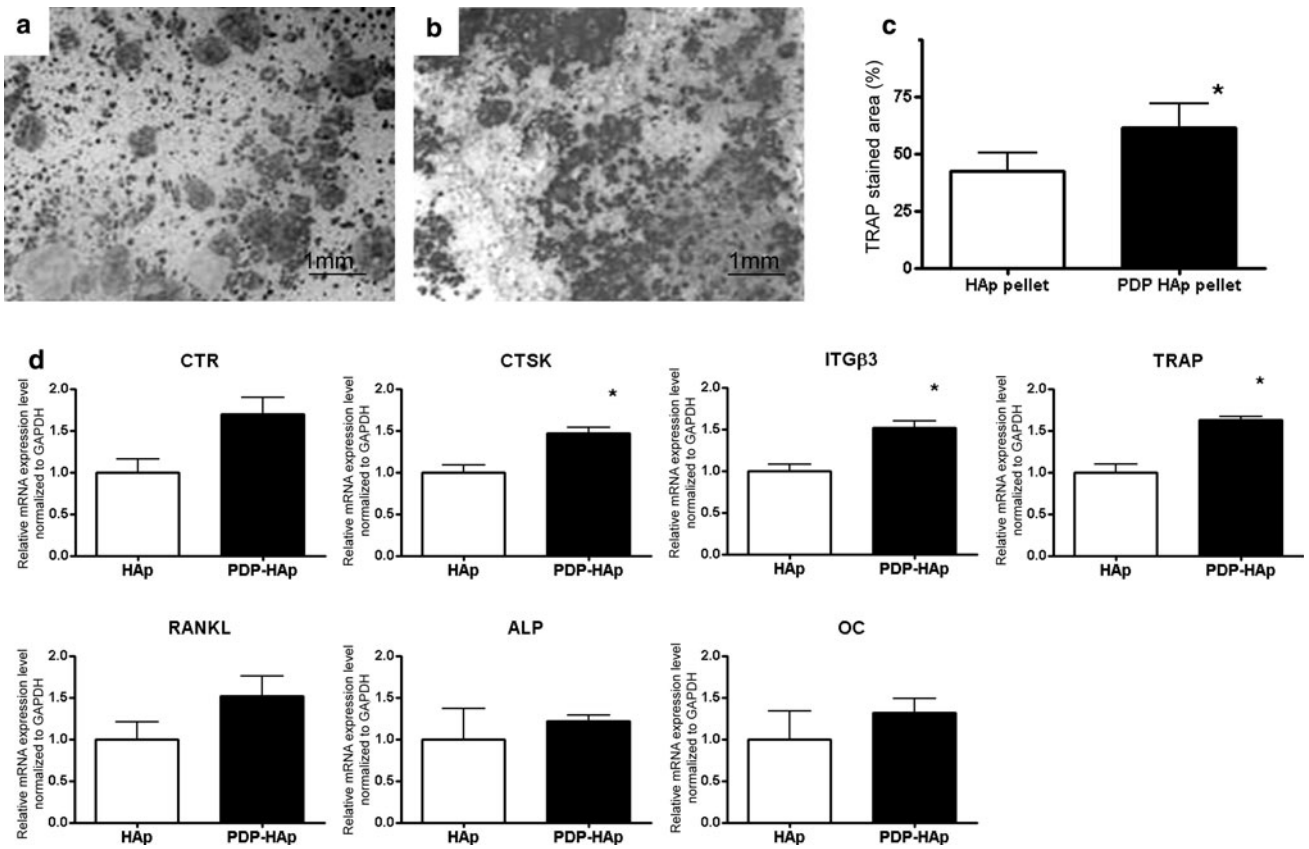

Fig. 2 In vitro osteoclastogenesis assay. Representative macroscopic photographs of the TRAP-stained surface of the HAp pellet (**a**) and PDP-HAp pellet (**b**) after 12 days of culture. Measurement of the TRAP-stained area (**c**) revealed that the surface of the PDP-HAp pellet induced higher bone absorption. mRNA expression of osteoclast- and osteoblast-related genes at 12 day of the culture is presented in (**d**). Expression of osteoclast-related genes (CTR, CTSK, ITGβ3, and TRAP) were higher in the PDP-HAp pellet compared with those of the HAp pellet. RANKL expression exhibited a similar trend to the osteoclast-related genes. Osteoblast-related genes (ALP and OC) manifested similar expression between HAp and on PDP-HAp. Data are expressed as mean ± SD. *$P < 0.05$ vs. HAp disc

TRAP-staining areas indicate both ceramics resorption pits and osteoclasts. The ratio of the TRAP-staining area to the total area of the PDP-HAp pellet was significantly larger than that of the HAp pellet (Fig. 2c).

3.2 mRNA expression of osteoclast and osteoblast marker genes

The mRNA expression of all osteoclast-related genes (CTR, CTSK, ITGβ3, and TRAP) were higher in the PDP-HAp pellet than in the HAp pellet (Fig. 2d). RANKL expression exhibited a similar trend, though it was likely expressed in osteoblasts or other mesenchymal cells. The expression of osteoblastic marker genes ALP and OC were slightly higher in cells cultured on PDP-HAp pellet than in those on HAp pellet; however, there was no significant difference between them.

3.3 Material properties of PDP-treated porous HAp

SEM micrographs revealed that PDP treatment did not alter the macroporous structure of HAp but it dramatically changed the microstructure (Fig. 3). The microporosity of the macropore walls increased and nanoscale grains of HAp crystals were deposited onto the surface of the large grains in the PDP-HAp. In contrast, the original HAp was composed of homogenously large grains of HAp crystals. The undecalcified histology, likewise, revealed similarities in macropore size and distribution between the PDP-HAp and original HAp (Fig. 6; Table 2).

3.4 Micro-CT evaluation

Micro-CT photographs revealed that both HAp and PDP-HAp integrated with the surrounding host bone after 4 weeks. HAp retained its original shape and volume through the observation period up to 16 weeks post surgery, whereas PDP-HAp gradually decreased in volume and its edges were rounded in the two-dimensional photographs with time (Fig. 4).

3.5 Histological findings

At 4 weeks after implantation, abundant bone ingrowth was observed in both HAp and PDP-HAp (Fig. 5a, d). At this time point, many TRAP-positive multinuclear osteoclasts were observed inside both HAp and PDP-HAp. A number of osteoclasts directly bound to the surface of the material were particularly found in the PDP-HAp specimens (Fig. 5b, e). At 16 weeks after implantation, the bone volume inside the implant decreased and bone marrow space became yellow marrow in the HAp; however, the amount of bone tissue remaining inside the implant was higher in the PDP-HAp than in the HAp (Fig. 5c, f). TRAP-positive osteoclasts were still observed inside both the HAp and PDP-HAp implants at 16 weeks, but the number of osteoclasts decreased compared with those at 4 weeks.

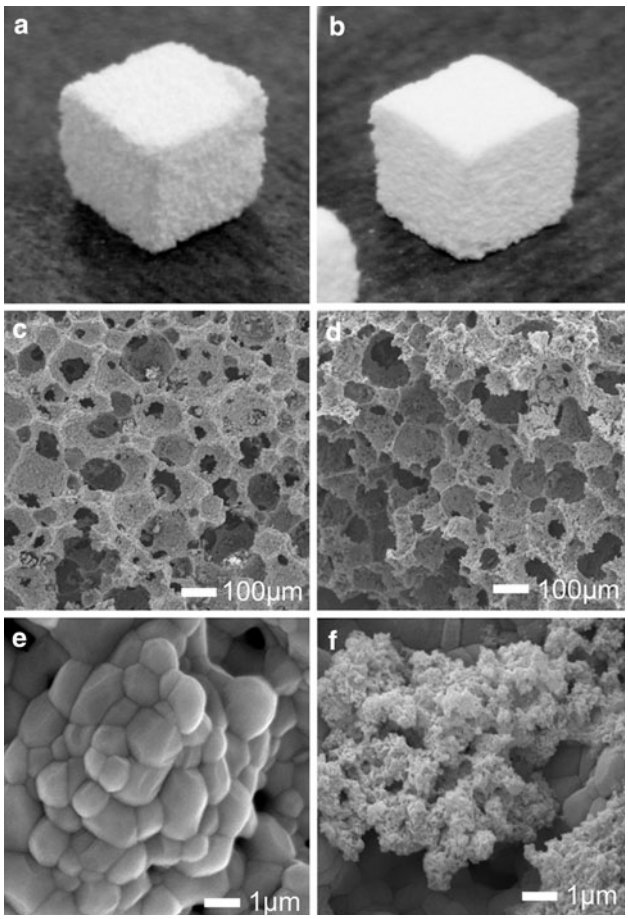

Fig. 3 Appearance and details of porous HAp and PDP-HAp for the in vivo experiment. Photographs (**a**, **b**) and SEM micrographs (**c**–**f**) of the HAp (**a**, **c**, **e**) and PDP-HAp (**b**, **d**, **f**). Lower magnification SEM micrographs (**c**, **d**) revealed that the macroporous structures of HAp and PDP-HAp were similar, but the PDP-HAp had more micropores on the macropore wall compared with HAp. Higher magnification photographs (**e**, **f**) demonstrated that the surface of PDP-HAp is covered with nanosized crystal grains, whereas HAp consisted of uniform, considerably larger grains

3.6 Histomorphometry

The results of histomorphometry are presented in Table 2. As demonstrated in Fig. 6, HAp.Ar/T.Ar decreased in the PDP-HAp group from 4 to 16 weeks post surgery (24% decrease from 4 to 16 weeks, $P < 0.05$), while HAp.Ar/T.Ar did not change in the HAp group. With decrease in the volume of material, pore size of PDP-HAp increased from four to 16 weeks. No significant change in HAp.Ar/T.Ar and pore size were observed from preimplantation up

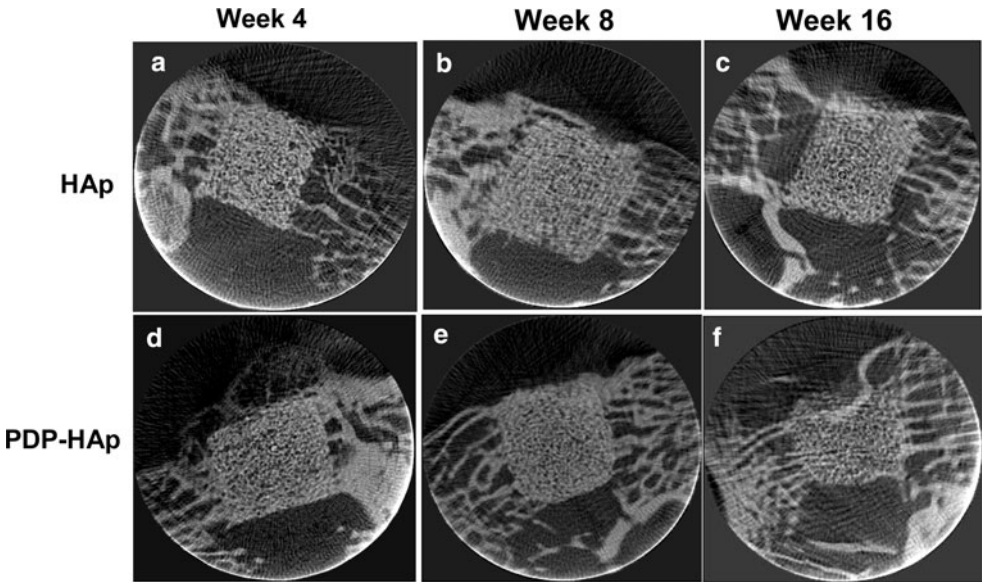

Fig. 4 Micro-CT photographs of the grafted region of rabbit femur. Representative axial images of the specimen implanted with either HAp (**a**–**c**) or PDP-HAp (**d**–**f**) at 4 weeks (**a**, **d**), 8 weeks (**b**, **e**), and 16 weeks (**c**, **f**) post operation. Both HAp and PDP-HAp were closely integrated with the host bone at 4 weeks after the surgery. HAp implant maintained its original shape through up to 16 weeks post operation, whereas the PDP-HAp implant became smaller and rounded with time

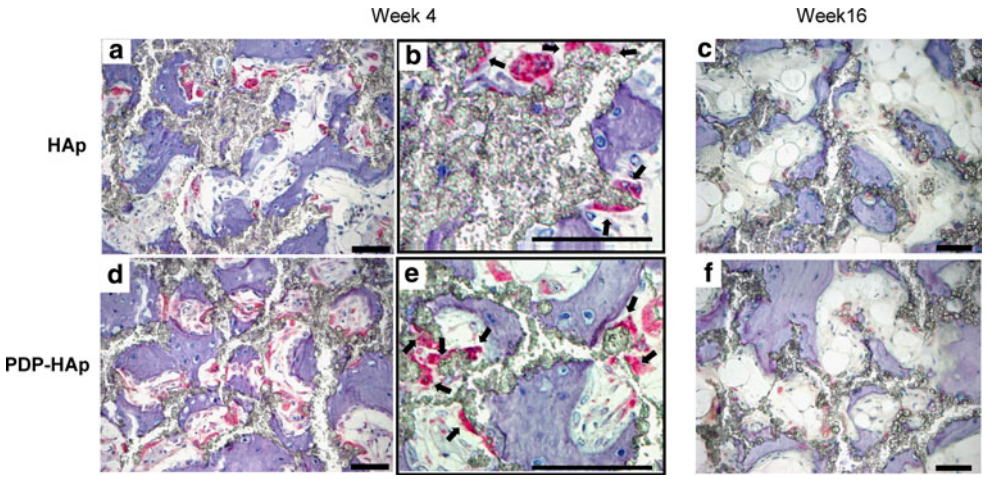

Fig. 5 TRAP-stained histological micrographs of the grafted material. **a**–**c** are the representative photographs of the central region of the HAp specimens at 4 weeks (**a**, ×40; **b**, ×200) and 16 weeks after surgery (**c**, ×40). **d**–**e** are the representative photographs of the central region of the PDP-HAp specimens at 4 weeks (**d**, ×40; **e**, ×200) and 16 weeks after surgery (**f**, ×40). Abundant osteoclasts, as well as bone ingrowth were seen at 4 weeks post operation and fewer osteoclasts were seen at 16 weeks post operation in both HAp and PDP-HAp. More osteoclasts were observed in PDP-HAp than in HAp at 4 weeks, and majority of them were directly attached onto the material (*arrows*). *Bar* = 100 μm

to week 4. B.Ar./T.Ar., which represents the amount of bone ingrowth, was similar in both PDP-HAp and HAp groups at 4 weeks post operation. B.Ar./T.Ar. decreased from 4 to 16 weeks post operation in the HAp group ($P < 0.05$), whereas it was maintained until 16 weeks in the PDP-HAp group (Fig. 6). B.C.S/T.S., which reflects the integration of material into the surrounding bone, exhibited a similar trend to that of B.Ar./T.Ar. N.Oc was significantly higher in the PDP-HAp group than in the HAp group at 4 weeks. N.Oc was generally higher in PDP-HAp than in HAp at 16 weeks, but no significant difference was observed between them.

4 Discussion

Even though highly porous HAp with interconnected pores promote the infiltration of bone tissue and vessels through the HAp, it remains less attractive as allogenic bone grafts because of its minimal bioabsorption, as well as its deficit in biologic activity. Therefore, various attempts have been made to improve HAp bioabsorbability. Composite materials made of HAp and other bioabsorbable materials such as collagens have been proposed as a solution to this problem [14–17]. PDP treatment, however, has certain advantages over the composite materials. First, PDP-

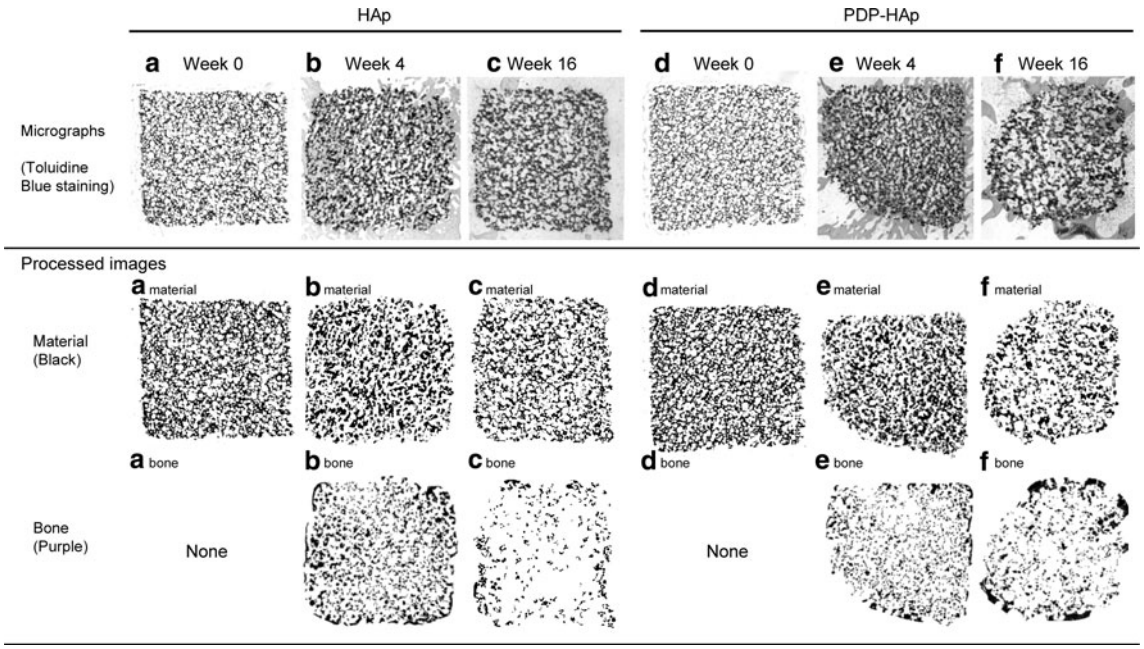

Fig. 6 Histological photographs of whole grafted material and processed images for histomorphometry. **a–f** present the representative microscopic photographs of the undecalcified sections of HAp (**a–c**) and PDP-HAp (**d–f**) stained with Toluidine blue before implantation (**a**, **d**), at 4 weeks (**b**, **e**), and at 16 weeks (**c**, **f**) after implantation. Each photograph covers the whole grafted material. **a–f**$_{material}$ and **a–f**$_{bone}$ are processed images of the HAp material and bone areas, respectively. These images are based on color difference using the ImageJ imaging software. In the original light micrographs, the HAp material is shown in *black* and bone in *purple*

Table 2 Histomorphometrical analysis of HAp and PDP-HAp implanted area (mean ± SD)

Parameters	Week 0 (before implantation)		Week 4		Week 16	
	HAp	PDP-HAp	HAp	PDP-HAp	HAp	PDP-HAp
Hydroxyapatite area/total area (%)	29.6 ± 2.8	29.9 ± 1.8	31.5 ± 4.5	30.3 ± 6.2	30.0 ± 7.1	22.9 ± 3.1*,#
Average pore size (diameter in μm)	160.92 ± 6.02	162.50 ± 3.07	164.51 ± 9.71	161.11 ± 6.86	163.35 ± 8.24	182.05 ± 7.24*,#
Bone area/total area (%)	None	None	27.9 ± 5.3	25.7 ± 8.1	14.9 ± 5.8#	24.0 ± 4.2*
Bone contact surface/total surface (%)	None	None	43.5 ± 10.7	39.3 ± 12.3	27.2 ± 11.70#	40.6 ± 4.2*
Number of osteoclasts (N.Oc;/mm^2)	None	None	53.83 ± 24.76	105.51 ± 29.55*	6.20 ± 5.84	7.86 ± 5.41

* $P < 0.05$ compared with that in HAp at same time point; # $P < 0.05$ compared with that at week 0

treatment is very simple and does not require specialized equipment. Second, it can be applied to any type of calcium phosphate material, including commercially available synthetic HAp [10]. Finally, this treatment can be performed at extremely low cost compared to the production of composite materials. Cost-effectiveness is definitely important because the financial capacity of patients determine treatment their choices, especially considering the recent medical economic policy.

This study has shown that the bioabsorbability of synthetic HAp could be improved through PDP-treatment. Although PDP-HAp was not completely absorbed (24% reduction in volume at 16 weeks), the histological findings suggest that its partial degradation enhanced physiological bone regeneration. As shown in the previous studies [18], HAp induces abundant bone ingrowth until four weeks after implantation. However, the bone tissue, once formed inside the material, remodeled and decreased in volume from 4 to 16 weeks. On the other hand, the amount of bone tissue formed inside the material was maintained in PDP-HAp from 4 to 16 weeks. These results suggest that gradual replacement with bone tissue resulted in physiologic bone remodeling in and around the PDP-HAp.

The reason for the incomplete degradation of PDP-HAp can be attributed to the mode of PDP-treatment. PDP-treatment modifies only the surface layer of HAp crystals and the deep layer of the HAp crystals retain their original property. Therefore, dense, compactly arranged HAp crystals in the deeper layer of the PDP-HAp resists degradation for at least 16 weeks. Despite these observations, these large, densely oriented HAp crystals may eventually be degraded in the body. Yamasaki et al. demonstrated that

highly porous synthetic HAp, similar to the HAp used in this study, was slowly degraded after 12 weeks post operation and was reduced to half the initial volume at 48 weeks post operation in rabbit models [18].

PDP-HAp is possibly degraded through two mechanisms, one is osteoclast-mediated and the other is dissolution-mediated [3, 4, 6, 7, 11, 18–23]. Although the osteoclast-mediated bioabsorption of ceramic materials is not completely understood, recent studies suggest that the micropore structure may stimulate osteoclast activity to enhance HAp bioabsorption [6, 11, 12, 24]. Yamasaki et al. demonstrated that HAps with micropores are degraded gradually, whereas those without micropores remained intact up to 48 weeks in rabbit models [18]. In contrast to the results of their study, HAp was not degraded at 16 weeks post surgery; however, the macropore wall of the HAp used in this study has micropores. On the other hand, the PDP-treated HAp, which had nanoscale grains deposited surface and more micropores on the macropore wall, increased osteoclast proliferation and apparent material degradation, indicating that surface microstructure affects osteoclastic activity. Although this study does not include how the PDP treatment enhanced osteoclast differentiation and function, the observed increase in RANKL expression in the osteoblasts suggests that osteoblasts recognized the surface geometry of HAp and mediated osteoclast activation.

Dissolution-mediated degradation may be improved by PDP-treatment. The degree of crystallinity affects the solubility behavior of apatite [7, 25, 26]. Highly crystalline apatite is generally insoluble, whereas poorly crystalline apatite is relatively soluble. Consequently, the surface layer of the PDP-HAp, composed of low crystalline apatite, may dissolve after implantation.

This study has a number of limitations. First, alterations in the mechanical strength of the implant during the postoperative course were not assessed. Given that both HAp and PDP-HAp were closely integrated with the surrounding bone tissue and that PDP-HAp degraded with time, measuring the mechanical strength of graft material is difficult. Moreover, the scaffold type HAp is mechanically weak and designed for use in non-weight bearing sites. However, measuring the time course change in strength of the bone region containing the implant and regenerated bone may prove useful. Second, although the results of the in vitro experiment were consistent with those of the in vivo experiment in terms of osteoclast behavior, care must be taken when interpreting the in vitro results. To compare the osteoclast activity between HAp and PDP-HAp, dense HAp pellets were used instead of porous HAp because the osteoclast number and absorption pits area are difficult to measure in scaffold-type materials. Furthermore, the PDP treatment of the dense HAp pellet was performed with a relatively short dissolution time because longer dissolution times could form pits on the HAp surface. Therefore, the results of the in vitro experiment may not accurately reflect in vivo cell behavior in PDP-HAps made from highly porous HAp.

In conclusion, this study suggests that PDP-treatment could enhance the bioabsorbability and degradability of synthetic HAp through cell-mediated and solution-mediated processes. PDP-treatment could likewise improve the integration of HAp into bone by facilitating its replacement with biological bone. Although PDP-HAp ceramics are unlikely to be degraded completely, its improved bioabsorbability and superior osteointegration compared with the untreated synthetic HAp are encouraging for its clinical use as a bone graft substitute.

Acknowledgments We are grateful for the material fabrication by Mr. Katsuo Nakamura of Hokkaido Industrial Research Institute, and participation in the soft X-ray and micro-CT study by Dr. Kazuharu Irie of the Health Sciences University of Hokkaido. Likewise, we wish to extend our gratitude to Hoya Co., Tokyo, Japan for supplying us with APACERAM AXTM porous HAp and CELLYARDTM HAp pellets.

References

1. Tamai N, Myoui A, Tomita T, Nakase T, Tanaka J, Ochi T, et al. Novel hydroxyapatite ceramics with an interconnective porous structure exhibit superior osteoconduction in vivo. J Biomed Mater Res. 2002;59(1):110–7. doi:10.1002/jbm.
2. Woodard JR, Hilldore AJ, Lan SK, Park CJ, Morgan AW, Eurell JA, et al. The mechanical properties and osteoconductivity of hydroxyapatite bone scaffolds with multi-scale porosity. Biomaterials. 2007;28(1):45–54.
3. Okuda T, Ioku K, Yonezawa I, Minagi H, Kawachi G, Gonda Y, et al. The effect of the microstructure of beta-tricalcium phosphate on the metabolism of subsequently formed bone tissue. Biomaterials. 2007;28(16):2612–21.
4. Okuda T, Ioku K, Yonezawa I, Minagi H, Gonda Y, Kawachi G, et al. The slow resorption with replacement by bone of a hydrothermally synthesized pure calcium-deficient hydroxyapatite. Biomaterials. 2008;29(18):2719–28.
5. Walsh WR, Vizesi F, Michael D, Auld J, Langdown A, Oliver R, et al. Beta-TCP bone graft substitutes in a bilateral rabbit tibial defect model. Biomaterials. 2008;29(3):266–71. S0142-9612(07)00788-0 [pii].
6. Chazono M, Tanaka T, Kitasato S, Kikuchi T, Marumo K. Electron microscopic study on bone formation and bioresorption after implantation of beta-tricalcium phosphate in rabbit models. J Orthop Sci. 2008;13(6):550–5. doi:10.1007/s00776-008-1271-1.
7. LeGeros RZ. Biodegradation and bioresorption of calcium phosphate ceramics. Clin Mater. 1993;14(1):65–88.
8. Leventouri T. Synthetic and biological hydroxyapatites: crystal structure questions. Biomaterials. 2006;27(18):3339–42.
9. Ben-Nissan B, Chai C, Evans L. Crystallographic and spectroscopic characterization and morphology of biogenic and synthetic apatites. In: Wnek G, Bowlin G, editors. Encyclopedia of biomaterials and biomedical engineering. 2nd ed. New York: Informa Healthcare USA; 2008. p. 191–221.
10. Akazawa T, Murata M, Takahata M, Ding X, Abe Y, Nakamura K, et al. Characterization of microstructure and bio-absorption of

the hydroxyapatite ceramics modified by a partial dissolution-precipitation technique using supersonic treatment. J Ceram Soc Jpn. 2010;118(6):535–40.
11. Akazawa T, Murata M, Sasaki T, Tazaki J, Kobayashi M, Kanno T, et al. Biodegradation and bioabsorption innovation of the functionally graded bovine bone-originated apatite with blood permeability. J Biomed Mater Res A. 2006;76(1):44–51. doi:10.1002/jbm.a.30439.
12. Murata M, Akazawa T, Tazaki J, Ito K, Sasaki T, Yamamoto M, et al. Blood permeability of a novel ceramic scaffold for bone morphogenetic protein-2. J Biomed Mater Res B Appl Biomater. 2007;81(2):469–75. doi:10.1002/jbm.b.30686.
13. Kartsogiannis V, Ng KW. Cell lines and primary cell cultures in the study of bone cell biology. Mol Cell Endocrinol. 2004;228(1–2):79–102. S0303-7207(04)00258-8 [pii].
14. So K, Fujibayashi S, Neo M, Anan Y, Ogawa T, Kokubo T, et al. Accelerated degradation and improved bone-bonding ability of hydroxyapatite ceramics by the addition of glass. Biomaterials. 2006;27(27):4738–44. S0142-9612(06)00461-3 [pii].
15. Nishikawa T, Masuno K, Tominaga K, Koyama Y, Yamada T, Takakuda K, et al. Bone repair analysis in a novel biodegradable hydroxyapatite/collagen composite implanted in bone. Implant Dent. 2005;14(3):252–60. 00008505-200509000-00010 [pii].
16. Schopper C, Ziya-Ghazvini F, Goriwoda W, Moser D, Wanschitz F, Spassova E, et al. HA/TCP compounding of a porous CaP biomaterial improves bone formation and scaffold degradation—a long-term histological study. J Biomed Mater Res B Appl Biomater. 2005;74(1):458–67. doi:10.1002/jbm.b.30199.
17. Shikinami Y, Matsusue Y, Nakamura T. The complete process of bioresorption and bone replacement using devices made of forged composites of raw hydroxyapatite particles/poly l-lactide (F-u-HA/PLLA). Biomaterials. 2005;26(27):5542–51.
18. Yamasaki N, Hirao M, Nanno K, Sugiyasu K, Tamai N, Hashimoto N, et al. A comparative assessment of synthetic ceramic bone substitutes with different composition and microstructure in rabbit femoral condyle model. J Biomed Mater Res B Appl Biomater. 2009;91(2):788–98. doi:10.1002/jbm.b.31457.
19. Hasegawa M, Doi Y, Uchida A. Cell-mediated bioresorption of sintered carbonate apatite in rabbits. J Bone Joint Surg Br. 2003;85(1):142–7.
20. Gonda Y, Ioku K, Shibata Y, Okuda T, Kawachi G, Kamitakahara M, et al. Stimulatory effect of hydrothermally synthesized biodegradable hydroxyapatite granules on osteogenesis and direct association with osteoclasts. Biomaterials. 2009;30(26):4390–400.
21. Rumpel E, Wolf E, Kauschke E, Bienengraber V, Bayerlein T, Gedrange T, et al. The biodegradation of hydroxyapatite bone graft substitutes in vivo. Folia Morphol (Warsz). 2006;65(1):43–8.
22. Lu J, Descamps M, Dejou J, Koubi G, Hardouin P, Lemaitre J, et al. The biodegradation mechanism of calcium phosphate biomaterials in bone. J Biomed Mater Res. 2002;63(4):408–12. doi:10.1002/jbm.10259.
23. Goto T, Kojima T, Iijima T, Yokokura S, Kawano H, Yamamoto A, et al. Resorption of synthetic porous hydroxyapatite and replacement by newly formed bone. J Orthop Sci. 2001;6(5):444–7.
24. Yokozeki H, Hayashi T, Nakagawa T, Kurosawa H, Shibuya K, Ioku K. Influence of surface microstructure on the reaction of the active ceramics in vivo. J Mater Sci Mater Med. 1998;9(7):381–4.
25. Fulmer MT, Ison IC, Hankermayer CR, Constantz BR, Ross J. Measurements of the solubilities and dissolution rates of several hydroxyapatites. Biomaterials. 2002;23(3):751–5.
26. Layrolle P, Daculsi G. Physicochemistry of apatite and its related calcium phosphates. In: Leon B, Jansen J, editors. Thin calcium phosphate coatings for medical implants. New York: Springer; 2009. p. 9–24.